

# Development of parallel microwave analysis code: ADVENTURE\_FullWave

Amane Takei

Department of Electrical and System Engineering, University of Miyazaki, 1-1 Gakuen Kibanadai-Nishi  
Miyazaki, 889-2192, Japan

E-mail: [takei@cc.miyazaki-u.ac.jp](mailto:takei@cc.miyazaki-u.ac.jp)

[www.miyazaki-u.ac.jp/english/](http://www.miyazaki-u.ac.jp/english/)

## Abstract

With the expansion of electromagnetic field analysis using computers, large spaces that include complex shapes have also become an analysis target, and the development of a high-accuracy analysis is required for these problems. Therefore, in the present study, Berenger's PML, which is currently the most effective absorbing boundary condition, is applied to the parallel finite element method based on the domain decomposition method, which is an effective analysis method for the microwave band. As a basic study, we developed an analysis code: ADVENTURE\_FullWave using a parallel finite element method based on the iterative domain decomposition method. In verifying the accuracy of the analysis code, we analyzed TEAM Workshop Problem 29, which is a benchmark problem, and confirmed that a highly accurate solution is obtained. Next, a model with Berenger's PML added to the dipole antenna model is used as an analysis object, and the absorption performance of the PML is evaluated using a reflection coefficient based on the S parameter. Moreover, the accuracy of the antenna analysis is evaluated by comparing the directivity of the dipole antenna with the theoretical solution.

*Keywords:* Iterative domain decomposition method, Parallel finite element method, Berenger's PML, Large-scale analysis, Microwave analysis.

## 1. Introduction

In the present study, Berenger's PML for the full-wave electromagnetic field analysis, which is currently regarded as the most effective absorbing boundary condition, is applied to the parallel finite element method, which is an analysis method that is capable of computing large-scale problems. We then show that the parallel finite element method is effective as an analysis method for a microwave band by calculating the problem dealing with an open domain and evaluating the solution's accuracy. First, as a basic study, we developed a three-dimensional electromagnetic field analysis solver using a parallel finite element method based on the iterative domain decomposition method. In order to verify the accuracy of the developed analytical solver, we calculate TEAM Workshop Problem 29, which is a benchmark problem, and evaluate the accuracy of the analytical solver. Next, a model with a PML added to the dipole

antenna is used as the analysis object, and the absorption performance of the PML is evaluated using a reflection coefficient based on the  $S$  parameter. Moreover, by comparing the directivity of the dipole antenna with the theoretical solution, evaluations of the accuracy and performance of the antenna analysis are performed. As a result, we confirmed the effectiveness of this method for microwave analysis.

## 2. Numerical analysis

We analyze TEAM Workshop Problem 29<sup>1</sup> in order to verify the accuracy of the developed analytical solver.<sup>2</sup> TEAM 29 is a benchmark problem and involves a resonator model. The resonator is cylindrical and has a diameter of 1.9 [m] and a height of 1.45 [m]. In the analysis, a dielectric phantom having a relative permittivity  $\epsilon_r$  of 80 and an electric conductivity  $\sigma$  of 0.52 [S/m] is positioned, and the resonance state is investigated. The analysis domain boundary is a perfect

conductor. The analysis model is shown in Fig. 1. Table 1 shows the specifications of the TEAM 29 model. The highest calculation efficiency is achieved when the number of elements contained in one subdomain is approximately 170, and the number of partial domains is determined such that the number of elements contained in one subdomain is equal to 170.

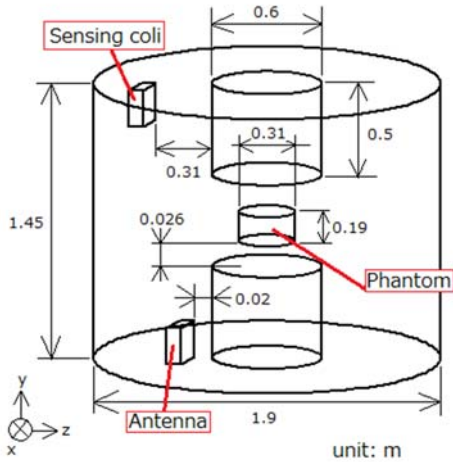


Fig. 1. TEAM 29 cavity resonator model

Table 1. TEAM 29 model data.

No. of Elements	DOFs	No. of Subdomains
121,277	149,668	100×7

The results of the analysis of TEAM 29 are subjected to frequency response analysis in order to confirm the accuracy of the developed analytical solver. In order to detect the resonant frequency and compare solutions with actual measurements, the frequencies of some range are analyzed. The frequency band of 60 [MHz] to 140 [MHz] is calculated for 2-MHz steps, and the response for every frequency step is investigated. In addition, calculations near the resonance frequency are performed in 0.4-MHz intervals. The computing environment used in the present study is a 25-PC cluster equipped with Intel Core i7-2600K multi-core CPUs (total: 100 cores) and 32 GB memory is used. The compiler used is the gcc. In addition, Message Passing Interface (MPI) is used for the parallelization library. The average calculation time per frequency step and the averagely used memory are shown in Table 2. Fig. 2 shows the frequency response of the

magnetic field. The measured and calculated values are shown in Table 3.

Table 2. Specifications of the TEAM 29 model.

No. of Elements	DOFs	No. of Subdomains
121,277	149,668	100×7

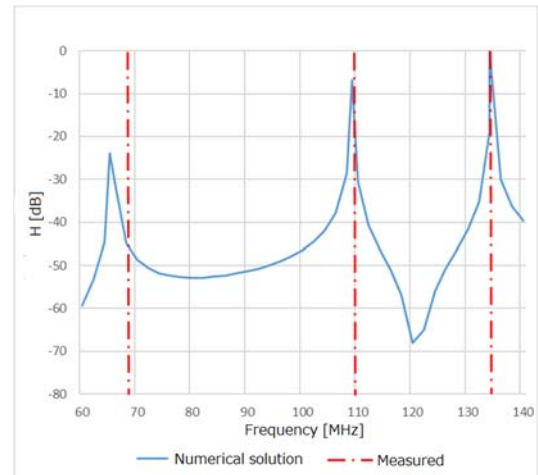


Fig. 2. Numerical and measured frequency response analysis results

Table 3. Resonance frequencies (Units: [MHz]. The error rate [%] between measured data and the numerical solution is shown in parentheses.)

Resonance mode	Measured data	FDTD 25-mm mesh	Result
1st	68.6	67 (2.33)	65.6 (4.37)
2nd	110	110	109.0 (0.91)
3rd	134	134	134.4 (0.30)

As shown in Fig. 2, a solution resonating around the resonance frequency of the actually measured value is obtained. In the comparison of the measured and calculated values, the error rate is 4.37 [%] in the 1st mode, 0.91 [%] in the 2nd mode, and 0.30 [%] in the 3rd mode. As the mode increases, the error rate decreases. However, it is the same tendency as the analysis result obtained by the FDTD method. Moreover, the error rate is less than 5 [%], and a solution with high accuracy is obtained.

Therefore, the solution obtained by the developed solver is proven to have a sufficiently high accuracy. Moreover,

in the analysis of the dipole antenna applying the PML described in the following sections, the error tolerance index is defined as 5 [%] in order to evaluate the accuracy.

### 3. PML

#### 3.1. Berenger's PML

The PML can be used to create an absorbing boundary by surrounding the analysis domain with a PML. From the viewpoint of the accuracy of the obtained solution, the PML is currently the most effective absorbing boundary condition. Although Berenger's PML is originally proposed as an absorbing boundary condition for the FDTD method, in the present study, we apply a finite element method dealing with an unstructured grid, we propose a simplified method omitting the directionality of electric conductivity given to the PML and confirm its effectiveness.

Berenger's PML stacks several PMLs outside the analysis domain and gradually sets a large value of electric conductivity according to the outer layer so that the outermost wall can be surrounded with a perfect conductor wall without reflecting electromagnetic waves. Fig. 3 shows a schematic diagram of Berenger's PML absorbing boundary.

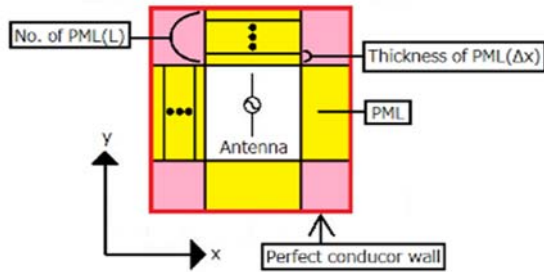


Fig. 3. PML absorbing boundary

In this paper the distribution of the electric conductivity for PML is expressed as follows:

$$\sigma = \sigma_{max} \left[ \frac{(L - \hat{L}(x)) \Delta x}{L \Delta x} \right]^M \quad (1)$$

where  $\Delta x$  is the thickness of PML 1,  $L$  is the number of layers of the PML,  $\hat{L}(x)$  is a coefficient determined by position  $x$ , and  $\hat{L}(x) = 0$  at the position of the  $L$ th layer,

$\hat{L}(x) = 1$  at the position of the  $(L-1)$ th layer, and  $\hat{L}(x) = L - 1$  at the position of the first layer.

Moreover,  $\sigma_{max}$  is the maximum value of the electric conductivity for the PML, and  $M$  is the degree distribution of electric conductivity. This equation is used to determine the electric conductivity of each layer of the PML.

The parameters to be determined as the parameters of the PML are the thickness  $\Delta x$  of PML 1, the number  $L$  of PML layers, the maximum electric conductivity  $\sigma_{max}$  of the PML, the degree  $M$  distribution of the electric conductivity, the reflection coefficient  $R$  [dB] between the PML of the outermost layer, and the perfect conductor wall. The reflection coefficient  $R$  is approximated as follows:

$$|R(\phi)| \cong \exp \left[ -\frac{2\sigma_{max}L\Delta x}{(M+1)\epsilon_0 c} \cos \phi \right] \quad (2)$$

where  $\phi$  is the incident angle of the electromagnetic wave, and  $c$  is the speed of light. Since we cannot decide the incident angle for an arbitrary incident wave,  $\phi = 0$ , a reflection coefficient for perpendicular incidence is used as a reference. Moreover, since the  $M$  that gives the distribution of the electric conductivity causes the calculation accuracy to deteriorate if the change of the electric field in the PML is too steep,  $M$  is approximately 2 to 4. If the number of layers  $L$  is too large, more memory will be required, and if  $L$  is too small, it will not function adequately as an absorbing boundary. There are many cases where the concrete number of  $L$  is set to 4 to 16. The thickness  $\Delta x$  of PML 1 is a constant thickness of all layers.

We set the reflection coefficient  $R(0)$  according to the required accuracy. Upon determining the above parameters, the maximum electric conductivity  $\sigma_{max}$  is given as follows:

$$\sigma_{max} = -\frac{(M+1)\epsilon_0 c}{2L\Delta x} \ln|R(0)| \quad (3)$$

In the present study, we construct a PML using (1) through (3) with  $L = 9$ ,  $M = 4$ , and  $\Delta x = \lambda/10$ . However, in order to reduce the analysis scale, we examine the optimum value of  $L$  in the next section.

### 3.2. Numerical results

We assign the PML to the dipole antenna model. The analysis domain is a cube of length 0.6 [m] so that the distance from the antenna to the innermost PML matches the wavelength. The current density is applied to the antenna as a current source as follows:

$$I(y) = I_0 \cos\left(\frac{2\pi}{\lambda}y\right) \quad : -l \leq y \leq l \quad (4)$$

where  $I_0 = 0.08$  [A/m<sup>2</sup>],  $\lambda$  is the wavelength, and  $l$  is the length from the feeding point to the antenna tip.

The analysis frequency is 1 [GHz], and the length of the antenna is 0.15 [m], which is the half wavelength. Here, mesh division is performed so that the maximum side length of the element is 1/20 of the wavelength. The analysis domain's boundary is a perfect conductor. Fig. 4 shows a schematic diagram of the dipole antenna model.

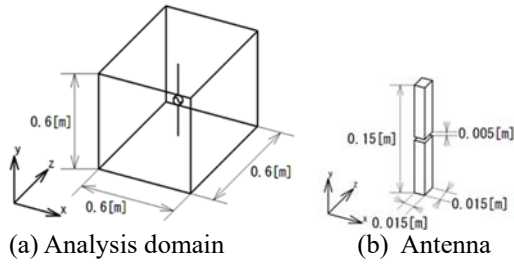


Fig. 4. Dipole antenna model

We assign PMLs to the domain boundary as shown in Fig. 4(a). The plane portion of the PML at the domain boundary overlaps a number of flat plates according to the number of layers, and the corner portion of the PML is one rectangular parallelepiped or cube. The boundary of the outermost layer of the PML is a perfect conductor wall. We perform performance evaluation by setting the thickness of one layer to be 0.03 [m] and the PML to have  $L = 9$  (hereinafter a PML with  $L$  layers is abbreviated as PML( $L$ )). Table 4 lists the number of elements and the degree of freedom of the analysis model.

Table 4. Number of elements and DOFs of the dipole antenna model

	PML(0): Perfect conductor wall	PML(9)
No. of Elements	4,669,759	26,899,669
DOFs	5,506,368	31,703,550

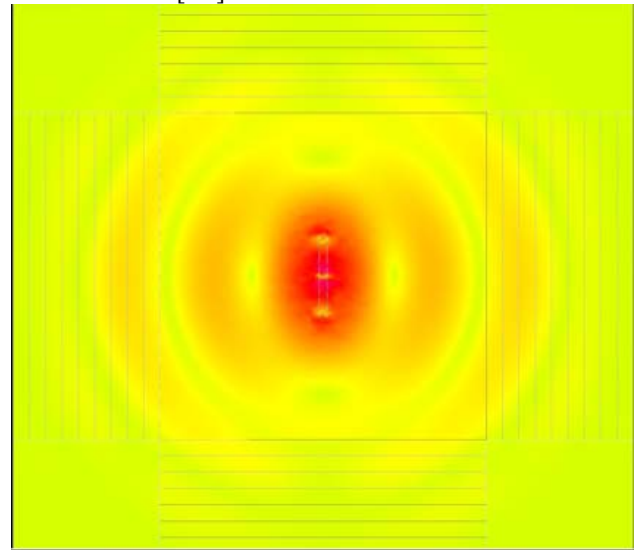
In (3), we set  $L = 9$ ,  $\Delta x = 0.03$ ,  $M = 4$ , and  $R(0) = -120$  [dB], which yields the maximum electric conductivity  $\sigma_{max}$  to PML(9). In addition, we decide the electric conductivity of each layer using (1). In this study, we set

the average value of each layer to the electric conductivity of the corner portion. We evaluate the performance of the PML based on the reflection coefficient obtained using the  $S_{11}$  parameter<sup>3</sup>. The observation point of the  $S_{11}$  parameter is on the x-axis 1 cm inside of the PML. The computing environment is the same as in the section 2. Table 5 lists the reflection coefficient, the CPU time, and the memory size.

Table 5. Results for reflection coefficient, CPU time, and memory size

	PML(0): Perfect conductor wall	PML(9)
Reflection coefficient [dB]	0	-18.65
CPU time [s]	1,278	18,787
Memory size [MB/core]	44.3	227.3

When the domain boundary is PML(0), i.e., when it is a perfect conductor wall,  $S_{11} = 1$ , so that the reflection coefficient is 0 [dB].



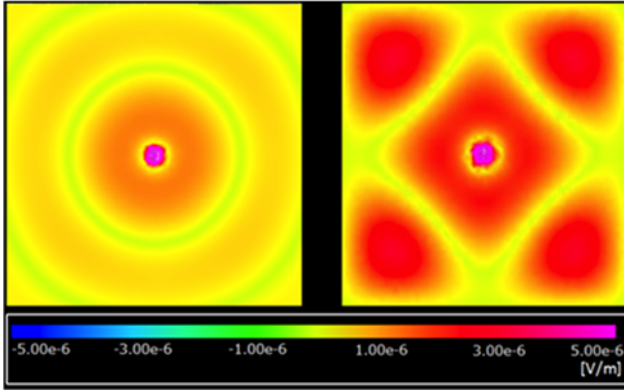


Fig. 5. Visualization of the analysis result (electric field) (Upper: Side view of with PML of PML(9), Lower-Left: Upper view of PML(9), L-Right: Upper view of PML(0))

On the other hand, when the domain boundary is PML(9), the reflection coefficient is -18.65 [dB]. The design target reflection coefficient of the antenna, for example, is generally approximately -10 to -20 [dB], and in the present study, we use a reflection coefficient of approximately -10 to -20 [dB]<sup>3</sup>. Thus, PML(9) can obtain sufficient absorption performance.

On the other hand, in comparing with PML (0), PML (9) increases the amount of memory used and computation time, depending on the absorbing layer applied. Fig. 7 shows a visualization diagram of the electric field obtained by analysis.

In Fig. 5, the left-hand side shows PML(9) at the boundary edge and the electric field propagates from the dipole antenna to the free space. On the other hand, the right-hand side of Fig. 5 shows the mode when the dipole antenna is enclosed by a perfect conductor wall.

Next, we perform the directivity evaluation of the dipole antenna by error evaluation using the theoretical solution in the far field. The error evaluation of the far field uses the E plane.

The theoretical solution<sup>3</sup> of the far field of the E plane is as follows:

$$E_{\theta} = j60I \frac{e^{-jkr}}{r} \cdot \frac{\cos\left(\frac{\pi}{2} \cos \theta\right)}{\sin \theta} \quad (5)$$

where  $j$  is the imaginary unit,  $I$  is the current, and  $r$  is the distance from the feeding point. The approximate distance  $r$  to the far-field peak of the Fresnel's region ( $2l^2/\lambda < r$ ) is 0.250 [m], if the dimension  $l$  ( $= 0.150$  [m]) of the dipole antenna is not ignored. Moreover,  $k$  is the wave number and is given by  $k = 2\pi/\lambda$ . The directivity evaluation is performed by comparing the

numerical analysis solution with the theoretical solution on the E plane. Fig. 6 shows a plot of the numerical analysis solution  $e_{\theta}$  and the theoretical solution  $E_{\theta}$  in increments of 1 [deg].

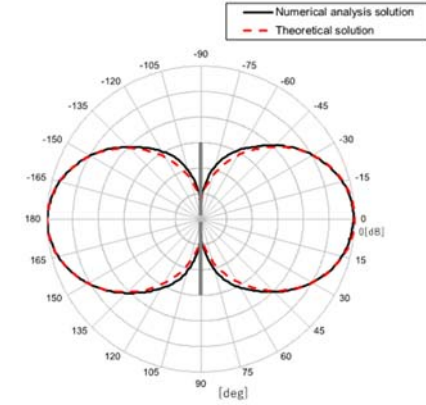


Fig. 6. Numerical and theoretical solutions in the E plane

The directivities of the numerical and theoretical solutions agree very well. The range of  $\theta$ , which is the far field far beyond the Fresnel's region, can be expressed by (6). The lower limit  $\theta_{Min}$  is  $\arcsin(2l^2/r\lambda) + 90 \cong -57$  [deg], and the upper limit  $\theta_{Max}$  is  $90 - \arcsin(2l^2/r\lambda) \cong 53$  [deg]. The average error rate  $E_{err}$  in this range is obtained by (7). As a result, the average error rate is 1.70 [%], and it is shown that a highly accurate solution can be obtained.

$$\arcsin\left(\frac{2l^2}{r\lambda}\right) + 90 \leq \theta \leq 90 - \arcsin\left(\frac{2l^2}{r\lambda}\right) \quad (6)$$

$$E_{err} = \frac{\sum_{i=\theta_{Min}}^{\theta_{Max}} \frac{|e_i - E_i|}{E_i}}{\theta_{Max} - \theta_{Min} + 1} \times 100 \quad [\%] \quad (7)$$

In the calculations shown in Fig.5, we used a dipole antenna model with PML(9). Here, we find the optimum  $L$  from the average error rate in the far field and the reflection coefficient of PML( $L$ ) by a parameter study using the number of PMLs. The computing environment is the same as in the section 2. Table 6 shows the number of elements for each  $L$ , the number of degrees of freedom of the edge, the error rate, the reflection coefficient, the calculation time, and the number of iterations of the COCG method applied to the interface problem.

Table 6. Numerical model data and results

PML(9)	PML(8)	PML(7)
--------	--------	--------

No. of elements	26,899,669	24,184,687	21,533,641
DOFs	31,703,550	28,506,352	25,383,890
Average error rate [%]	1.70	3.81	12.87
Reflection coefficient [dB]	-18.65	-15.79	-15.04
CPU time [h]	5.22	3.77	2.81
No. of iterations	46,508	37,755	30,695
Memory size [MB/core]	227.3	204.6	182.6

From Table 6, PML(9) is the case with the best far field accuracy. When the allowable range of the error rate is less than 5 [%], which is the allowable range of numerical analysis error, since PML(7) has a reflection coefficient of less than -15 [dB], the PML functions sufficiently. However, the error rate exceeded the allowable range. We can find that PML(8) is optimal because it has a better calculation time and iteration count than PML(9).

#### 4. Conclusion

In the present paper, we propose a simplified method that omits the directionality to Berenger's PML for the full-wave electromagnetic field analysis and gives the average value of the electric conductivity of each layer at the corner of the model. Performance evaluation reveal that sufficient absorption performance can be obtained. In the accuracy verification by directivity evaluation of the dipole antenna, when the maximum element side length is set to 1/20 of the wavelength and the PML to be given is set to 9 layers, the error rate of the numerical solution and the theoretical solution is about 1.70 [%]. It is found that a highly accurate solution can be obtained. In addition, when the tolerance range of the far-field error rate that is considered to be sufficiently practical is set to less than 5 [%], an eight-layer PML is found to be optimal. In addition, the usefulness of the proposed method for a frequency band of 1.2 GHz or higher, which is used in microphones and mobile phones, is demonstrated.

#### Acknowledgements

The present study was supported in part by a JSPS Grant-in-Aid for Scientific Research (Basic Research (B), 17H03256). The computer environment used in the

present study was supported in part through a JST Adaptable and Seamless Technology transfer Program (A-STEP (Search Type), AS262Z02631H).

#### References

1. TEAM Workshop, Tucson, AZ, USA, 1998.
2. A. Takei, S. Sugimoto, M. Ogino, S. Yoshimura, H. Kanayama: Full Wave Analyses of Electromagnetic Fields with an Iterative Domain Decomposition Methodm, IEEE Transactions on Magnetics, 46:8 (2010), 2860-2863.
3. Fujikura LTD. Homepage: <http://www.fujikura.co.jp/eng/>